2002

Hybridization and Bond-Orbital Components in Site-Specific X-Ray Photoelectron Spectra of Rutile TiO_2

J. C. Woicik

E. J. Nelson

See next page for additional authors

Citation/Publisher Attribution

Woicik, J. C., Nelson, E. J., Kronik, L., Jain, M., Chelikowsky, J. R., Heskett, D., Berman, L. E., & Herman, G. S. (2002). Hybridization and Bond Orbital Components in Site Specific X-Ray Photoelectronic Spectra of Rutile TiO_2. *Physical Review Letters*. *89*(7), 077401. doi: 10.1103/PhysRevLett.89.077401
Available at: https://doi.org/10.1103/PhysRevLett.89.077401

Hybridization and Bond-Orbital Components in Site-Specific X-Ray Photoelectron Spectra of Rutile TiO_2

J. C. Woicik,[1] E. J. Nelson,[1] Leeor Kronik,[2] Manish Jain,[2] James R. Chelikowsky,[2] D. Heskett,[3] L. E. Berman,[4] and G. S. Herman[5]

[1]*National Institute of Standards and Technology, Gaithersburg, Maryland 20899*
[2]*Department of Chemical Engineering and Materials Science, University of Minnesota, Minneapolis, Minnesota 55455*
[3]*Department of Physics, University of Rhode Island, Kingston, Rhode Island 02881*
[4]*National Synchrotron Light Source, Upton, New York 11973*
[5]*Hewlett-Packard Company, Corvallis, Oregon 97330*

(Received 3 December 2001; published 26 July 2002)

We have determined the Ti and O components of the rutile TiO_2 valence band using the method of site-specific x-ray photoelectron spectroscopy. Comparisons with calculations based on pseudopotentials within the local density approximation reveal the hybridization of the Ti $3d$, $4s$, and $4p$ states, and the O $2s$ and $2p$ states on each site. These chemical effects are observed due to the large differences between the angular-momentum dependent matrix elements of the photoelectron process.

DOI: 10.1103/PhysRevLett.89.077401 PACS numbers: 78.70.Dm, 79.60.–i, 82.80.Ej

X-ray photoelectron spectroscopy (XPS) has provided much direct and important information pertaining to the occupied electronic density of states for many materials [1]. However, because XPS measures the transition probabilities between the initial, bound-state valence electrons and the final, continuum-state photoelectrons, the technique does not render the density of occupied electronic states. Rather, it produces the density of these states modulated by the electronic transition-probability matrix elements [1]:

$$I(E, h\nu) \propto \sum_{i,l} \rho_{i,l}(E)\sigma_{i,l}(E, h\nu)\,. \qquad (1)$$

Here E is the photoelectron binding energy, $h\nu$ is the x-ray photon energy, $\rho_{i,l}(E)$ are individual, angular-momentum l resolved, electronic single-particle partial density of states of the ith atom of the crystalline-unit cell, and $\sigma_{i,l}(E, h\nu)$ are the angle-integrated, angular-momentum dependent, photoionization cross sections.

Here we employ the newly developed technique of site-specific x-ray photoelectron spectroscopy [2] to determine the individual Ti and O contributions to the rutile TiO_2 valence band. Comparisons with state-of-the-art, *ab initio* local density approximation (LDA) calculations of the Ti and O partial density of states demonstrate the importance of the individual angular-momentum components of the crystal-valence band and their direct relevance to the solid-state electronic structure.

The experiment was performed at the National Synchrotron Light Source using the National Institute of Standards and Technology beam line X24A. The double-crystal monochromator was operated with Si(111) crystals, and high-resolution photoelectron spectra were obtained with a hemispherical electron analyzer. Atomically clean, stoichiometric single-crystal rutile $TiO_2(110)$ surfaces were prepared by 500 eV Ar sputtering followed by annealing in 7×10^{-7} torr of O_2 at 650 °C. All spectra were recorded with the photon beam incident to the (110) surface at 45°.

The calculations were performed by using *ab initio* Troullier-Martins pseudopotentials within the local density approximation using a plane-wave basis [3]. Pseudopotentials based on electronic configurations of $3s^2 3p^6 4s^0 3d^2$ (Ti) and $2s^2 2p^4$ (O) were used, with $s/p/d$ (Ti) and s/p (O) cutoff radii (in atomic units) of 2.3/1.5/2.25 and 1.45/1.45, respectively. A plane-wave cutoff energy of 120 Ry and a $4 \times 4 \times 6$ Monkhorst-Pack k-point sampling scheme were used to guarantee convergence. We obtained values of $a = 4.57$ Å, $c/a = 0.643$, and $u = 0.303$ for the structural parameters of the rutile TiO_2 phase, which are in excellent agreement with the experimental values of $a = 4.59$ Å, $c/a = 0.644$, and $u = 0.305$ [4]. All calculated curves have been convolved with a Gaussian of width 0.4 eV to simulate the total experimental resolution.

The valence-photoelectron spectrum recorded off of the Bragg condition ($h\nu \sim 2695$ eV) is shown in Fig. 1. It is compared to the *ab initio* LDA calculation of the total electronic density of states. (The curve labeled "c theory" is addressed below.) The curves have been scaled to equal peak height and referenced to the valence-band maximum. The LDA calculation may seem to reproduce the experimental photoemission density of states curve adequately; however, this agreement is fortuitous. In fact, careful inspection of the data and calculation reveals a poor energy alignment and a poor agreement on the widths of the two lobes characteristic of the rutile photoelectron spectrum [5].

In order to establish the origins of these discrepancies, the individual Ti and O components of the rutile valence band were obtained from the experimental photoelectron

 0031-9007/02/89(7)/077401(4)$20.00

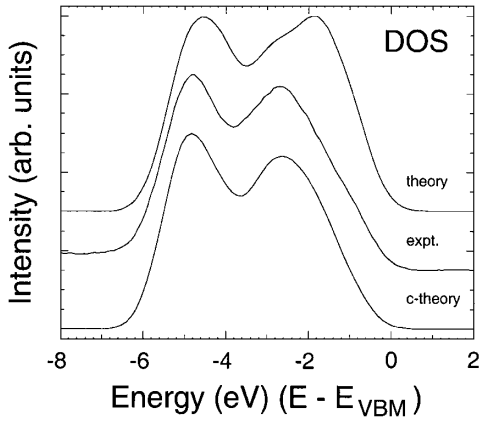

FIG. 1. Theoretical total electronic density of states (upper curve), the valence-photoelectron spectrum recorded off of the Bragg condition (middle curve), and the theoretical total electronic density of states corrected for individual Ti and O angular-momentum dependent photoelectron cross sections (lower curve). The curves have been scaled to equal peak height.

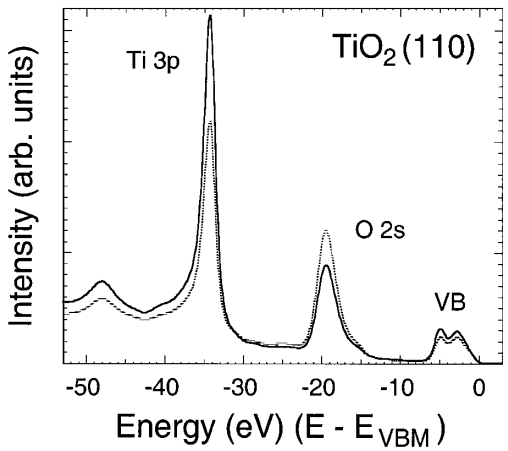

FIG. 2. Photoelectron spectra from the rutile $TiO_2(110)$ surface recorded within the photon-energy width of the $TiO_2(200)$ Bragg back-reflection condition. The photon energies were chosen to maximize the electric-field intensity on either the Ti (solid curve) or O (dotted curve) atomic plane.

spectra of Fig. 2. These spectra have been recorded at two different photon energies within the photon-energy width ($\Delta E \sim 0.38$ eV) of the rutile $TiO_2(200)$ Bragg back-reflection condition ($h\nu \sim 2700$ eV) that were chosen to maximize the electric-field intensity on either the Ti or O atomic plane. The well known x-ray standing-wave effect [6] is observed for the Ti $3p$ and O $2s$ core lines, as well as for the crystal-valence band. The spectra were aligned relative to the energy position of the Ti $3p$ core line and normalized to the electric-field intensity at either the Ti or O atomic position that was taken as the intensity of the Ti $3p$ or O $2s$ core line, respectively. After removal of an integrated background from the valence-band region, linear combinations of the two spectra yielded the *experimental* photoemission partial density of state curves [2] around the Ti and O sites, as shown in Fig. 3.

Clearly, the large contribution of Ti to the valence-band spectrum indicates significant covalent bonding between the Ti and O atoms, despite the formal Ti^{4+} charge state of Ti in rutile. (Had Ti been completely ionized, there would be no Ti valence-electron emission.) Although early interpretations of the rutile TiO_2 photoelectron spectrum have attributed the valence-electron emission primarily to the O $2p$ derived valence states [5], our data support more recent resonant-photoemission [7,8], x-ray photoelectron-diffraction [8], and x-ray fluorescence studies [9] that have indicated a significant amount of Ti $3d$ (and possibly $4s$) admixture in the valence band.

In order to understand the implications of these findings, theoretical Ti and O partial density of state curves, also shown in Fig. 3, were calculated by projecting the obtained wave functions over the Ti and O valence atomic orbitals within spheres centered around the Ti and O atoms. The use of finite sphere radii produces the theoretical site specificity, and the sphere radii were chosen to be equal to the known covalent radii of each species, $\sim$1.3 Å for Ti and $\sim$0.75 Å for O.

Clearly, agreement between theory and experiment is much less than satisfactory, and it is significantly worse than had been suggested by Fig. 1. In particular, the second lobe of the Ti valence band is nearly absent in the theory, and the triply peaked structure of the O valence band is poorly reproduced. Furthermore, it is clear that no weighted linear combination of the theoretical Ti and O partial density of states, attempting to account for the

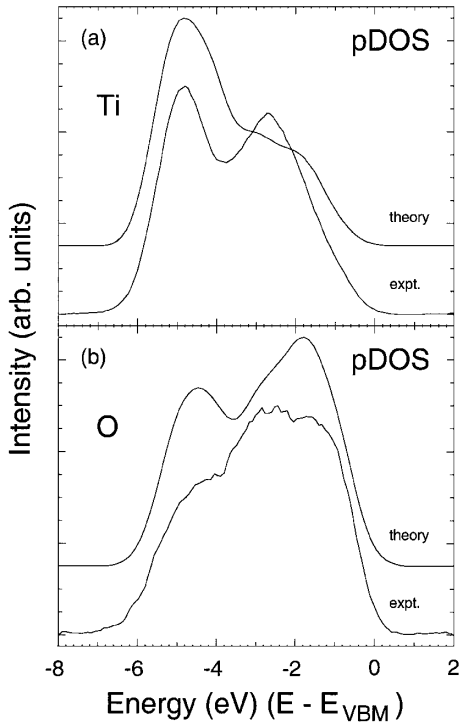

FIG. 3. Theoretical partial density of states and the experimental site-specific valence-photoelectron spectrum: (a) Ti; (b) O. Theoretical and experimental curves have been scaled to equal peak height. The O component has been scaled by a factor of 4 relative to the Ti component.

different photoelectron cross sections of the dominant Ti $3d$ and O $2p$ orbitals, would produce a more accurate representation of the experimental data. Additionally, x-ray fluorescence studies, that, unlike XPS, sample states of particular angular momenta, have revealed the presence of Ti states in addition to Ti $3d$ and an O $2p$ structure that is only doubly peaked [9]. For these reasons, the theoretical Ti and O partial density of states were decomposed into their angular-momentum resolved components. These curves are shown in Fig. 4. It is clear that the second lobe of the experimental Ti spectrum cannot be reproduced without inclusion of the Ti $4p$ component, and the intermediate structure of the experimental O spectrum cannot be reproduced without inclusion of the O $2s$ component.

Drawing on the physical insight gleaned from Eq. (1), we modeled the partial density of states curves from the weighted sums of the different orbital components of Fig. 4 using the tabulated theoretical atomic cross sections (Ti $\sigma_{4s}/\sigma_{3d} \sim 9.9$ and O $\sigma_{2s}/\sigma_{2p} \sim 29$) [10]. Agreement between the theoretical and experimental partial density of states was much improved; however, even better agreement was obtained for both the Ti and O components if the relative atomic cross sections were scaled by an additional factor of 2. We note that up to a full 1.5 of this factor of 2 could come from the choice of theoretical deconvolution radii in addition to changes in the valence wave functions in going from the atomic to the solid state. The resulting theoretical *corrected* partial density of states are shown in Fig. 5, together with the experimental data. The agreement now between theory and experiment is startling, and we note that this agreement has been achieved without any energy dependence of the cross sections across the energy width of the valence band or the consideration of many-body effects.

We may now recalculate the total density of states from the theoretical corrected Ti and O partial density of states using the *experimental* Ti and O *total* cross sections determined from the areas of the individual Ti and O components of the rutile valence band ($\mathrm{Ti_{VB}}/\mathrm{O_{VB}} \sim 3.4$). Figure 1 compares the resulting theoretical corrected total density of states with the photoelectron spectrum recorded off of the Bragg condition. Clearly, the agreement between theory and experiment is no longer fortuitous.

At this point, it is instructive to consider the molecular orbitals for an octahedral transition-metal oxide containing a first-row transition metal [11], although the octahedral (O_h) symmetry around the cation is usually slightly distorted [12]. In this depiction, the metal $4s$ orbitals bond with the ligand σ orbitals to form the $a_{1g}(\sigma^b)$ level, the metal $3d_{x^2-y^2}$ and $3d_{z^2}$ orbitals bond with the ligand σ orbitals to form the $e_g(\sigma^b)$ level, the metal $4p$ orbitals bond with both the ligand σ and π orbitals to form the $t_{1u}(\sigma^b)$ and $t_{1u}(\pi^b)$ levels, and the metal $3d_{xy}$, $3d_{xz}$, and $3d_{yz}$ orbitals bond with the ligand π orbitals to form the $t_{2g}(\pi^b)$ level. Additionally, there are ligand π orbitals

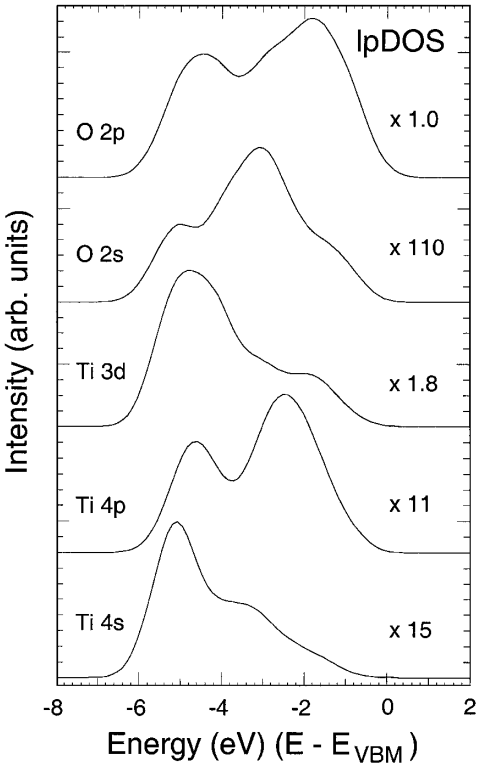

FIG. 4. The different *angular-momentum* components of the theoretical Ti and O partial density of states. Multipliers relative to the O $2p$ component are indicated in each case.

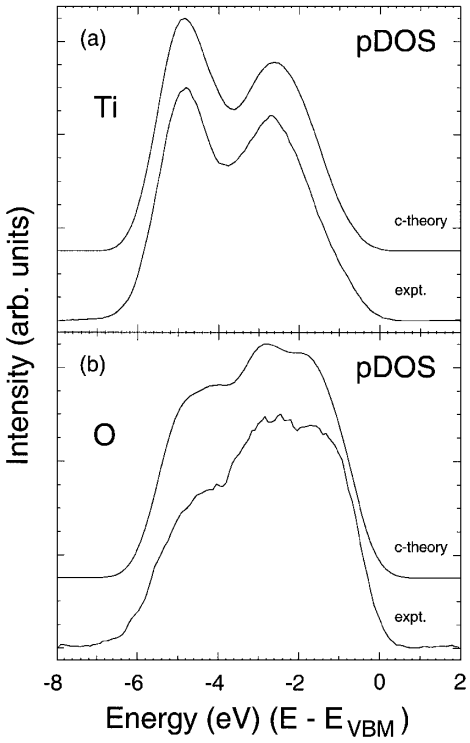

FIG. 5. Theoretical partial density of states corrected for individual angular-momentum dependent photoelectron cross sections and the site-specific experimental valence-photoelectron spectrum: (a) Ti; (b) O. The curves have been scaled to equal peak height.

$[t_{1g}(\pi)$ and $t_{2u}(\pi)]$ that are left over and are rigorously nonbonding in O_h symmetry.

Examination of both the experimental partial density of states and the theoretical corrected partial density of states of Fig. 5 leads to an attractive interpretation of the electronic structure within this σ and π bonding scheme. The doubly lobed Ti structure of the valence band may be attributed to the energy splitting between the σ and π groupings of the bonding states, with the σ bonds lying at the lower energy [11]. These states are mirrored in the triply lobed O structure, and they occur at the same energy as in the Ti spectrum, indicating the sharing of electrons in a covalent bond. The O nonbonding π states then naturally compose the third lobe of the O spectrum; they occur at higher energy than the O bonding π states and reveal little or no electron density on the metal atoms, as expected. Close inspection of the angular-momentum resolved components of Fig. 4 supports these conclusions, although the solid-state electronic structure is much more complicated than the electronic structure of an octahedral TiO_6 molecule. In particular, the groupings of the orbitals into discrete σ and π states is not as transparent, and the effect of translational symmetry spreads the states into bands (Bloch functions). Additionally, metal-metal and ligand-ligand interactions that are not present in isolated molecules are known to affect the valence electronic structure [13].

It is instructive to examine the hybridization of the metal and ligand orbitals within this bonding scheme. As both the O $2s$ and $2p_z$ atomic orbitals belong to the same symmetry representation of the O_h point group, the ligand σ orbitals will contain a mixture of these states [11]; i.e., $|\psi_{L,\sigma}\rangle = \alpha|2s\rangle + \sqrt{1-\alpha^2}\,|2p_z\rangle$. (The ligand π orbitals are constructed solely from the O $2p_x$ and $2p_y$ atomic orbitals.) This hybridization orients the ligand-charge density towards the metal atoms, leading to an increased overlap between the metal and ligand wave functions. It has been stated by Mulliken that ''a little bit of hybridization goes a long way'' to stabilize a chemical bond [11], and, from the theoretical calculations of Fig. 4, we see that α, the mixing coefficient, is only $\sim$10%, even though the O $2s$ valence (or hybrid) component accounts for as much as $\sim$30% of the experimental O valence spectrum (due to the much larger cross section of the O $2s$ versus the O $2p$ atomic orbitals). This relatively small value of α results from the relatively large energy separation between the O $2s$ and $2p$ atomic orbitals that, as seen from the data in Fig. 2, is $\sim$17 eV. On the other hand, the energy separation between the Ti $3d$, $4s$, and $4p$ atomic orbitals is significantly smaller ($\sim$8 eV) [7,11], accounting for the much larger amount of Ti $3d$, $4s$, and $4p$ hybridization observed on the Ti sites.

Amusingly, it is the added complexity of the photoemission process, i.e., the ''overrepresentation'' of orbitals with smaller values of angular momenta (O $2s$ versus O $2p$, and Ti $4s$ and $4p$ versus Ti $3d$) that affords this observation of chemical hybridization in the solid-state electronic structure: the observation of σ and π bonds and of oxygen nonbonding states, and the positive identification of valence-band contributions from the O $2s$ and the Ti $4s$ and $4p$ orbitals.

This work was performed at the National Synchrotron Light Source, which is supported by the U.S. Department of Energy. Additional support was provided by the Computational Materials Science Network of the Department of Energy, the National Science Foundation, and the Minnesota Superconducting Institute.

[1] *Photoelectron Spectroscopy: Principles and Applications*, S. Hufner (Springer-Verlag, Berlin, 1996), 2nd ed.

[2] J. C. Woicik, E. J. Nelson, and P. Pianetta, Phys. Rev. Lett. **84**, 773 (2000); J. C. Woicik, E. J. Nelson, T. Kendelewicz, P. Pianetta, M. Jain, L. Kronik, and J. R. Chelikowsky, Phys. Rev. B **63**, R41403 (2001); J. C. Woicik, E. J. Nelson, D. Heskett, J. Warner, L. E. Berman, B. A. Karlin, I. A. Vartanyants, M. Z. Hasan, T. Kendelewicz, Z. X. Shen, and P. Pianetta, Phys. Rev. B **64**, 125115 (2001).

[3] K. M. Glassford and J. R. Chelikowsky, Phys. Rev. B **46**, 1284 (1992).

[4] S. C. Abrahams and J. L. Bernstein, J. Chem. Phys. **55**, 3206 (1971).

[5] S. Hufner and G. K. Wertheim, Phys. Rev. B **8**, 4857 (1973); S. P. Kowalczyk, F. R. McFeely, L. Ley, V. T. Gritsyna, and D. A. Shirley, Solid State Commun. **23**, 161 (1977); J. Riga, C. Tenret-Noel, J. J. Pireaux, R. Caudano, J. J. Verbist, and Y. Gobillon, Phys. Scr. **16**, 351 (1977).

[6] D. P. Woodruff, D. L. Seymour, C. F. McConville, C. E. Riley, M. D. Crapper, N. P. Prince, and R. G. Jones, Surf. Sci. **195**, 237 (1988); J. Zegenhagen, Surf. Sci. Rep. **18**, 199 (1993).

[7] Z. Zhang, S.-P. Jeng, and V. E. Henrich, Phys. Rev. B **43**, 12 004 (1991).

[8] R. Heise, R. Courths, and S. Witzel, Solid State Commun. **84**, 599 (1992).

[9] L. D. Finkelstein, E. Z. Kurmaev, M. A. Korotin, A. Moewes, B. Schneider, S. M. Butorin, J.-H. Guo, J. Nordgren, D. Hartmann, M. Neumann, and D. L. Ederer, Phys. Rev. B **60**, 2212 (1999).

[10] M. B. Trzhaskovskaya, V. I. Nefedov, and V. G. Yarzhemsky, At. Data Nucl. Data Tables **77**, 97 (2001). As the Ti $4p$ orbitals are unoccupied in the free Ti atom, the Ti $4p$ atomic cross section is not tabulated; consequently, we took it to be equal to the Ti $4s$ one. Additionally, the calculations have been performed for filled atomic subshells; therefore, in order to obtain the cross sections on a per-electron basis, they must be normalized by the orbital degeneracy which is equal to $2l + 1$.

[11] C. J. Ballhausen and H. B. Gray, *Molecular Orbital Theory* (Benjamin, New York, 1964), Chaps. 4 and 8. The ligand z axis is directed towards the metal ion.

[12] L. A. Grunes, R. D. Leapman, C. N. Wilker, R. Hoffmann, and A. B. Kunz, Phys. Rev. B **25**, 7157 (1982).

[13] C. Castellani, C. R. Natoli, and J. Ranninger, Phys. Rev. B **18**, 4945 (1978).